Synthesis, Characterization and Biological Evaluation of novel Ru(II)-Arene Complexes containing intercalating Ligands

Stefan Nikolić,[a,#] Loganathan Rangasamy,[b,#] Nevenka Gligorijević,[c] Sandra Aranđelović,[c] Siniša Radulović,[c] Gilles Gasser[b,*] and Sanja Grgurić-Šipka[a,*]

[a] *Faculty of Chemistry, University of Belgrade, Studentski trg 12-16, 11000 Belgrade, Serbia.*

[b] *Department of Chemistry, University of Zurich, Winterthurerstrasse 190, CH-8057 Zurich, Switzerland.*

[c] *Institute for Oncology and Radiology of Serbia, Pasterova 14, 11000 Belgrade, Serbia.*

[#] these authors have contributed equally to the work.

[*] corresponding authors: Email: gilles.gasser@chem.uzh.ch; WWW: www.gassergroup.com; Tel.: +41 44 635 46 30; Email: sanjag@chem.bg.ac.rs; WWW: www.chem.bg.ac.rs/osoblje/36-en.html; Tel: +381 11 3336 742.

Abstract

Three new ruthenium(II)-arene complexes, namely [(η^6-*p*-cymene)Ru(Me_2dppz)Cl]PF_6 (**1**), [(η^6-benzene)Ru(Me_2dppz)Cl]PF_6 (**2**) and [(η^6-*p*-cymene)Ru(aip)Cl]PF_6 (**3**) (Me_2dppz = 11,12-dimethyldipyrido[3,2-a:2',3'-c]phenazine; aip = 2-(9-anthryl)-1*H*-imidazo[4,5-*f*][1,10] phenanthroline) have been synthesized and characterized using different spectroscopic techniques including elemental analysis. The complexes were found to be well soluble and stable in DMSO. The biological activity of the three complexes was tested in three different human cancer cell lines (A549, MDA-MB-231 and HeLa) and in one human non-cancerous cell line (MRC-5). Complexes **1** and **3**, carrying η^6-*p*-cymene as the arene ligand, were shown to be toxic in all cell lines in the low micromolar/subnanomolar range, with complex **1** being the most cytotoxic complex of the series. Flow cytometry analysis revealed that complex **1** caused concentration- and time-dependent arrest of the cell cycle in G2-M and S phase in HeLa cells. This event is followed by the accumulation of the sub-G1 DNA content after 48 h, in levels higher than cisplatin and in the absence of phosphatidylserine externalization. Fluorescent microscopy and acridine orange/ethidium bromide staining revealed that complex **1** induced both apoptotic and necrotic cell morphology characteristics. Drug-accumulation and DNA-binding studies performed by inductively coupled plasma mass spectrometry in HeLa cells showed that the total ruthenium uptake increased in a time- and concentration-dependent manner, and that complex **1** accumulated more efficiently than cisplatin at equimolar concentrations. The introduction of a Me_2dppz ligand into the ruthenium(II)-*p*-cymene scaffold was found to allow for the discovery of a strongly cytotoxic complex with significantly higher cellular uptake and DNA-binding properties than cisplatin.

Keywords:

Anticancer Agents
Bioorganometallic Chemisty
DNA Intercalating Ligand
Medicinal Inorganic Chemistry
Ruthenium(II)-arene complex

1. Introduction

The majority of the anticancer chemotherapeutic treatments are based on platinum complexes (i.e. CDDP = *cis*-diamminedichloridoplatinum(II) better known as cisplatin, carboplatin and oxaliplatin) [1]. However, the use of these drugs is limited by their toxicity and acquired drug resistance [2]. These facts have initiated intensive research towards the discovery of novel metal-based drug candidates with better selectivity toward cancer cells [3, 4, 5, 6]. Among the different metals investigated for this purpose, ruthenium complexes have shown the greatest potential [7, 8]. For example, three Ru(III) complexes NAMI-A (trans-[tetrachlorido(1H-imidazole)(S-dimethyl sulfoxide) ruthenate(III)]), KP1019 (indazolium trans-[tetrachloridobis(1H-indazole) ruthenate(III)]), and KP1339 (sodium trans-[tetrachloridobis(1H-indazole)ruthenate(III)]) have entered human clinical trials [9, 10, 11, 12, 13, 14]. Two of them, namely NAMI-A and KP1339 are now in phase II clinical trial [15]. In addition, two Ru(II) complexes, namely RAPTA-C ([Ru(η^6-*p*-cymene)Cl_2(pta)]; pta = 1,3,5-triaza-7-phosphaadamantane) and TLD-1433 (as a photosensitizer in photodynamic therapy) should enter into clinical trials in the very near future [16, 17 ,18].

Despite these promising results with ruthenium compounds, the quest for novel lead structures is still a topic of high interest. Of particular interest are arene ruthenium complexes with σ-bonded aromatic ligands that can bind to DNA both by metal coordination or through intercalation of an attached aromatic ligand [19, 20, 21]. Such a concept was employed by Sadler and co-workers, who reported DNA intercalation of $[(arene)Ru(en)Cl]^+$ complexes where en is ethylenediamine and the arene ligands are biphenyl, 9,10-dihydroanthracene or 5,8,9,10-tetrahydroanthracene (Figure 1. **a-c**) [22]. Comparative analysis of Ru(II)-arene complexes containing tetrahydroanthracene (partial intercalation) or containing *p*-cymene (no intercalation) suggested that the complexes with an intercalating ligand have a stronger DNA mismatch repair protein inhibition [23] than the one which do not intercalate. In addition, it was found that the coordination of guanine to ruthenium may assist in the intercalation of the bulky tetrahydroanthracene ligand into DNA [24, 25, 26]. Of note, ruthenium(II)-benzene or ruthenium(II)-cymene derivatives coordinated to aryl imidazole and aryl benzimidazole were found to interact with DNA through binding and intercalation [27]. DFT calculation confirmed that large and flexible arene ligands are able to form more stabilizing intercalation interactions with DNA bases than small and less flexible arene ligands [28]. This concept was used in the

design of (arene)ruthenium(II) complexes of 1,3-dimethyl-4-acylpyrazolon-5-ato ligands where the arene is a monoaromatic ligand [29]. Docking studies of those complexes confirmed that increased aromaticity of the ligand is important for intercalation and π-π stacking interactions between the ligand and DNA base pairs (Figure 1. **d**). Worthy of note, Sheldrick *et al.* correlated the aromatic ring size with the cytotoxic properties of the resulting complexes (η^6-hexamethylbenzene)Ru(κ^2N-N)](CF_3SO_3), where N-N = phen (1,10-phenanthroline), tap (1,4,5,8-tetraazaphenanthrene), dpq (dipyridoquinoxaline = pyrazino[2,3-*f*][1,10]phenanthroline), dppz = dipyridophenazine, dppn = 4,5,9,16-tetraaza-dibenzo[*a,c*]naphthacene (Figure 1. **e**) [30, 31]. The authors observed that the cytotoxicity of the complexes was increasing with the size of the intercalating moiety. The same trend was observed in the case of [Ru(bpy)$_2$(N-N)]Cl_2 complexes when the N-N ligands bpy, phen, dpq, dppz and dppn were compared [32]. Also, a Ru(II)-benzene complex with a phenanthroimidazole derivative as the intercalative moiety was shown to damage DNA by intercalation in cancer cells (Figure 1. **f**) [33] and to stabilize *c-Myc* G-quadruplex DNA (G4-DNA) by affecting its conformation [34]. Interestingly, Ru(II)-cymene complexes with intercalating ligands such as phen, dppz and dppn also have luminescent properties, which can be used for diagnostic purposes [35]. Contrary to the examples presented above, intercalative ligands can sometimes be more toxic than the corresponding Ru(II)-arene complexes bearing those ligands [36]. Worthy of note, Ru(II)-arene complexes with ligands similar to nucleic bases, namely fluorouracil derivatives were also reported by Hu and co-workers [37]. Of note, ruthenium-arene complexes with intercalative ligands cannot not only used to help targeting DNA but also to enable the loading of such compounds into micelles to enhance drug efficacy and overcome drug resistance [38].

Taking into account the potential of the combination of a Ru-arene complex with an intercalative ligand, we decided to investigate the cytotoxicity of two different DNA intercalating moieties, namely 11,12-dimethyldipyrido[3,2-a:2',3'-c]phenazine (Me_2dppz) and 2-(9-anthryl)-1*H*-imidazo[4,5-*f*][1,10]phenanthroline (aip), with the Ru(II)-arene scaffold (Scheme 1.). Herein, we report on the synthesis, characterization and in-depth biological evaluation of three new "piano stool" ruthenium(II)-arene complexes, namely [(η^6-*p*-cymene)Ru(Me_2dppz)Cl]PF_6 (**1**), [(η^6-benzene)Ru(Me_2dppz)Cl]PF_6 (**2**) and [(η^6- *p*-cymene)Ru(aip)Cl]PF_6 (**3**).

Insert Figure 1

2. Experimental

2.1. Materials

All chemicals were of reagent-grade quality or higher, were obtained from commercial suppliers and were used without further purification. Solvents were used as received or dried over molecular sieves. $RuCl_3$ was purchased from I2CNS.

2.2. Instrumentation and methods

^1H and ^{13}C NMR spectra were recorded in deuterated solvents on a Bruker DRX 400 (^1H: 400 MHz, ^{13}C: 100.6 MHz), Bruker Ultrashield Advance III spectrometer 500 (^1H: 500 MHz, ^{13}C: 126 MHz) or Varian Gemini-200 (^1H: 200 MHz, ^{13}C: 50 MHz) MHz spectrometers at room temperature. The chemical shifts, δ, are reported in ppm (parts per million), and coupling constants (J) in Hertz. The residual solvent peaks have been used as an internal reference. The abbreviations for the peak multiplicities are as follows: s (singlet), d (doublet), dd (doublet of doublets), t (triplet), q (quartet), m (multiplet), and br (broad). ESI mass spectra were recorded on a Bruker Esquire 6000 spectrometer. Elemental microanalyses were performed on a LecoCHNS-932 elemental analyzer. Infrared spectra were recorded on a Nicolet 6700 FT-IR spectrometer using the ATR technique. Conductivity measurements were performed using a Crison MultiMeter MM41 instrument.

2.3. Synthesis

The ligand 11,12-dimethyldipyrido[3,2-a:2',3'-c]phenazine (Me_2dppz) was synthesized by condensation of 1,10-phenathroline-5,6-dione [39] with 4,5-dimethylbenzene-1,2-diamine according to a published procedure [40, 41]. The ligand2-(9-anthryl)-1*H*-imidazo[4,5-*f*][1,10] phenanthroline (aip) was prepared by condensation of the same dione with 9-anthraldehyde under conditions described in the literature [42]. The ruthenium dimers $[(\eta^6\text{-}p\text{-cymene})\text{-}RuCl_2]_2$ and $[(\eta^6\text{-benzene})\text{-}RuCl_2]_2$ were prepared according to a published procedure [43].

$[Ru(\eta^6\text{-}p\text{-cymene})(Me_2dppz)Cl]PF_6$ **(1)**

Me_2dppz (36 mg, 0.116 mmol) was dissolved in 5 mL of methanol and 5 mL of dichloromethane. To this solution, a solution of $[(\eta^6\text{-}p\text{-cymene})\text{-}RuCl_2]_2$ (35.5 mg, 0.058 mmol)

in 4 mL of dichloromethane was then added dropwise with constant stirring. The mixture was stirred at room temperature for 5 h and then filtered. NH_4PF_6 (28 mg, 0.174 mmol) was then added to the solution and left to stir over night at room temperature. The yellow precipitate, which formed, was filtered and washed with cold Et_2O, MeOH and dried in vacuo. Yield: 56.6 mg (64 %).

Elemental analysis: Calcd. for $C_{30}H_{28}ClF_6N_4PRu$ x $2H_2O$ C, 47.28; H, 4.23; N, 7.35. Found: C, 47.44; H, 3.83; N, 7.51. IR (cm^{-1}): 3648 (w), 3091 (w), 2971 (w), 1493 (w), 1471 (w), 1411 (w), 1359 (w), 840 (s), 729 (w), 558 (w). ^{1}H NMR (400 MHz, DMSO-d_6) δ 10.00 (d, J = 4.8 Hz, 2H), 9.55 (d, J = 8.0 Hz, 2H), 8.28 (dd, J = 7.6, 5.2 Hz, 2H), 8.10 (s, 2H), 6.40 (d, J = 6.0 Hz, 2H), 6.17 (d, J = 6.0 Hz, 2H), 2.71 (m, 1H), 2.59 (s, 6H), 2.24 (s, 3H), 1.01 (d, J = 6.8 Hz, 6H). ^{13}C NMR (100 MHz, DMSO-d_6) δ 157.00, 147.54, 143.93, 141.04, 138.07, 134.93, 129.41, 127.69, 127.46, 104.78, 102.64, 85.91, 84.22, 30.43, 21.74, 20.18, 18.21. ESI-MS (CH_3CN): *m/z* 581.2 ($[M\text{-}PF_6]^+$).

[Ru(η^6-benzene)(Me_2dppz)Cl]PF_6 **(2)**

To a solution of Me_2dppz (35 mg, 0.113 mmol) in 8 mL of dichloromethane was added a suspension of [(η^6-benzene)-$RuCl_2$]$_2$ (28 mg, 0.056 mmol) in 6 mL of methanol. The reaction mixture was stirred for 5 h at room temperature and filtered. NH_4PF_6 (27 mg, 0.168 mmol) was then added to the solution. The solution was then left to stir over night. The pale yellow precipitate, which formed, was filtered, washed with cold Et_2O, MeOH and dried in vacuo. Yield: 56.7 mg (73 %).

Elemental analysis: Calcd. For $C_{26}H_{20}ClF_6N_4PRu$ x H_2O C, 45.39; H, 3.22; N, 8.14. Found: C, 45.35; H, 3.061; N, 8.162. IR (cm^{-1}): 3097 (w), 2988 (w), 2942 (w), 1497 (w), 1442 (w), 1411 (w), 1356 (w), 833 (s), 731 (w), 556 (w). ^{1}H NMR (500 MHz, DMSO-d_6) δ 10.08 (dd, J = 5.5, 0.8 Hz, 1H), 9.54 (dd, J = 8.0, 1.0 Hz, 1H), 8.26 (dd, J = 6.8, 2.5, Hz, 1H), 8.09 (s, 1H), 6.39 (s, 6H), 2.58 (s, 6H). ^{13}C NMR (125 MHz, DMSO-d_6) δ 157.31, 147.59, 144.00, 141.08, 137.90, 134.99, 129.36, 128.30, 127.71, 127.31, 86.87, 20.18. ESI-MS (CH_3CN): *m/z* 525.1 ($[M\text{-}PF_6]^+$).

[Ru(η^6-*p*-cymene)(aip)Cl]PF_6 **(3)**

To a suspension of 2-(9-anthryl)-1*H*-imidazo[4,5-*f*][1,10]phenanthroline (aip) (30 mg, 0.075 mmol) in 5 mL of dichloromethane and 5 mL of methanol was added dropwise a solution of [(η^6-

p-cymene)-$RuCl_2]_2$ (23 mg, 0.038 mmol) in 5 mL of dichloromethane. The reaction mixture was stirred for 8 h at room temperature and then filtered. NH_4PF_6 (24.2 mg, 0.15 mmol) was then added to the solution. The solution was then left to stir for 2 h. The pale yellow precipitate, which formed, was filtered, washed with cold Et_2O and MeOH and dried in vacuo. Yield: 60.4 mg (94 %).

Elemental analysis: Calcd. For $C_{37}H_{34}ClF_6N_4O_2PRu$ x $2H_2O$ C, 52.39; H, 4.04; N, 6.61. Found: C, 51.85; H, 4.08; N, 6.64. IR (cm^{-1}): 3640 (w), 3060 (m), 2970 (m), 2930 (m), 1607 (w), 1544 (w), 1507 (w), 1447 (w), 1413 (w), 1365 (w), 839 (s), 742 (m), 556 (w). ^{1}H NMR (500 MHz, DMSO-d6) δ 14.83 (bs, 1H), 9.92 (d, J = 5.0 Hz, 2H), 9.19 (bs, 2H), 8.95 (s, 1H), 8.30 – 8.20 (m, 4H), 7.80 (d, J = 8.0 Hz, 2H), 7.61 (t, J = 7.0 Hz, 2H), 7.53 (s, 2H), 6.3 9 (d, J = 6.5 Hz, 2H), 6.15 (d, J = 6.0 Hz, 2H), 2.67 (m, 1H), 2.25 (s, 3H), 0.96 (d, J = 7.0 Hz, 6H).^{13}C NMR (125 MHz, DMSO-d6) δ 153.92, 150.66, 143.31, 132.44, 130.82, 130.64, 129.61, 128.64, 127.31, 126.39, 125.83, 125.49, 124.40, 104.02, 103.10, 86.23, 83.97, 30.46, 21.73, 18.33. ESI-MS (CH_3CN): *m/z* 667.2 ($[M\text{-}PF_6]^+$).

2.4. Bioassays

For the biological examination (intracellular accumulation, interactions with DNA, cytotoxicity), the complexes and corresponding ligands were dissolved in DMSO (20 mM) prior to use. DMSO solutions were mixed with the aqueous solutions used in biological studies immediately prior to use, so that the final concentration of DMSO never exceeded 0.1% (v/v).

2.5. Cell culture

Three human tumor cell lines: human cervix adenocarcinoma (HeLa), human alveolar basal adenocarcinoma (A549), human breast adenocarcinoma (MDA-MB-231), and one non-tumor human lung fibroblast cell line (MRC-5), were maintained as monolayer culture in nutrient medium, (Roswell Park Memorial Institute) RPMI-1640 (Gibco). RPMI-1640 medium was supplemented with 5% fetal calf serum (FCS, Gibco), 100 U mL^{-1} penicillin and 100 mg mL^{-1} streptomycin, 4-(2-hydroxyethyl)piperazine-1-ethanesulfonic acid (HEPES) (25 mM), L-glutamine (3 mM). The cells were grown at 37 °C, in 5% CO_2 and humidified air atmosphere.

2.6. Trypan blue exclusion assay

Trypan blue (TB) exclusion assay was used to determine the number of viable cells present in a cell suspension. TB test is based on the principle that viable cells possess intact cell membranes that exclude trypan blue dye, whereas non-viable cells do not. Staining was carried out following a previously described protocol [44]. Briefly, cell suspension (50 µL) was mixed with 250 µL of filtered TB solution (0.4%). Immediately after, cells were visually examined by light microscopy and cell number determined using a Neubauer chamber. Viable cells appear with clear cytoplasm, while non-viable appear with blue cytoplasm.

2.7. Cytotoxicity studies

The cytotoxicity of the compounds towards lung (A549), breast mammary gland (MDA-MB-231), cervix (HeLa) cancer cell lines and Normal Human Lung cells (MRC5) was measured by a fluorometric cell viability assay using resazurin (Promocell GmbH). Cells were plated in triplicates in 96-well plates at a density of ~5 x 10^3 cells/well in 100 µL 24 h prior to treatment. Cells were then treated with increasing concentrations of compounds for 48 h. After 48 h in the incubator, the medium was replaced by 100 µL medium containing resazurin (0.2 mg/mL final concentration). After 4 h of incubation at 37 °C, the fluorescence of the highly red fluorescent resorufin product was quantified at 590 nm emission with 540 nm excitation wavelength in a SpectraMax M5 microplate Reader.

2.8. Flow-cytometric analysis of cell cycle phase distribution

Quantitative analysis of cell cycle phase distribution was performed by flow-cytometric analysis of the DNA content in fixed HeLa cells, after staining with propidium iodide (PI) [45]. Cells were seeded at density of 2 x 10^5 cells per well, into 6-well plates (Thermo Scientific Nunc™), in 2 mL of nutrition medium. Cells were continually exposed to the investigated ruthenium complex **1** or CDDP at concentrations corresponding to IC_{50} and 2 x IC_{50}. Control cells were incubated only in nutrient medium. After 24 h or 48 h of growth, cells were collected, washed twice with ice-cold phosphate-buffered saline (PBS), and fixed overnight, in 70% ethanol. After fixation, cells were washed with PBS, and incubated with RNaseA (1 mg/mL) for 30 min, at 37 C. Immediately before flow-cytometric analysis, cells were stained with PI, at a concentration of 400 mg/mL. Cell cycle phase distribution was investigated using fluorescence

activated cell sorter (FACS), by Calibur Becton Dickinson flow cytometer, at 488 nm excitation line (Argon-ion laser). Collected data were analyzed by Cell Quest computer software.

2.9. Flow-cytometric analysis of apoptosis by Annexin-FITC

Quantitative analysis of apoptotic and necrotic cell death induced by complex **1**, was performed by Annexin-FITC (fluorescein isothiocyanate) apoptosis detection kit, according to the manufacturer's instructions (BD Biosciences). HeLa cells (2 x10^5) were seeded into 6-well plates (Thermo Scientific Nunc™), in 2 mL of RPMI medium. After 24 h of growth, cells were treated with complex **1** or CDDP, for 24 h and 48 h, at concentrations corresponding to their IC_{50} and 2 x IC_{50} values. Following treatment, cells were washed twice with ice-cold PBS and then resuspended in 200 µl binding buffer (10 mM HEPES/NaOH pH 7.4, 140 mM NaCl, 2.5 mM $CaCl_2$). 100 µl of cell suspension (10^5 cells) was transferred to a 5 mL culture tube and mixed with 5 µl of Annexin-FITC and 5 µl of propidium iodide (PI) [46]. Cells were vortexed and incubated for 15 min, at 25 °C in the dark. Afterwards, 400 µl of binding buffer was added to each tube and analyzed using a FACS Calibur Becton Dickinson flow cytometer and Cell Quest computer software.

2.10. Morphological analysis of cell death by fluorescent microscopy

HeLa cells (2 x 10^4) were seeded into 6-well plates (ThermoScientific Nunc™) in 2 mL of nutrient medium. After 24 h of growth, cells were exposed to complex **1** or CDDP, at IC_{50} or 2 x IC_{50} concentrations. Following 24 h or 48 h of treatment, cells were stained with ethidium bromide (5 µg/mL) and acridine orange (1.5 µg/mL), according to standard procedure [47], and immediately after, observed under the fluorescent microscope Axio Observer Z1, using AxioVision imaging software (Carl Zeiss MicroImaging GmbH).

2.11. Sample microwave digestion for ICP-MS

The digestion was performed on an Advanced Microwave Digestion System (ETHOS 1, Milestone, Italy) using HPR-1000/10S high pressure segmented rotor. The pressure-resistant PTFE vessels (volume 100 mL), which were used in this study, consisted of fluoropolymer liner. Before use, the PTFE vessels were acid cleaned and rinsed with ultra-pure water. This type of vessel permits a maximum temperature of 240 ºC and a maximum pressure of 100 bar.

Maximally, 10 PTFE vessels could simultaneously be mounted on the rotor. The internal temperature was monitored only with one vessel equipped with a sensor unit. Temperature sensor is over a sensor-protecting tube directly contacted with digested solution. The entire sample was precisely and quantitatively transferred, mixed in each clean vessel with 3 mL of HNO_3 (65%), 4 mL of ultra-pure water and 2 mL of H_2O_2 (30%) (Suprapure®, Merck, Germany) and then heated with microwave energy for 10 min. The temperature was controlled with a predetermined power program. The temperature was typically raised to 200 ºC in the first 10 min, and to a peak temperature of 200 ºC in the next 10 min, and then cooled down rapidly. After cooling and without filtration, the solution was diluted to a fixed volume into a 10 mL volumetric flask and made up to 10 mL volume with ultra-pure water. Ultra-pure water was prepared by passing doubly deionized water from Milli-Q system (Millipore, Bedford, MA, USA) to a resistivity of 18.2 MΩ·cm.

2.12. Measurement of intracellular ruthenium(II) and platinum(II) accumulation using ICP-MS

Intracellular accumulation of complex 1 was analyzed in HeLa cells, in comparison to CDDP, using inductively coupled plasma mass spectrometry (ICP-MS), using a Thermo Scientific iCAP Qc ICP-MS (Thermo Scientific, Bremen, Germany) [48] spectrometer with operational software Qtegra. The instrument was optimized for optimum performance in He KED (Kinetic Energy Discrimination) mode using the supplied autotune protocols. The ICP-MS instrument was tuned using a solution TUNE B iCAP Q (1 µg/L of each: Ba, Bi, Ce, Co, In, Li, U) provided by the manufacturer Thermo Scientific, Germany. External standards for the instrument calibration was prepared on the basis of ruthenium, plasma standard solution, Specpure®, Ru 1000µg/mL certified reference solution ICP Standard purchased from Alfa Aesar GmbH & Co KG (Germany). The acid concentration of the external standards was carefully matched to the acid concentration of the prepared samples. Two types of blanks are required for the analysis of the samples prepared. The calibration blank is used in establishing the analytical curve and the method blank is used to identify possible contamination resulting from either the reagents (acids) or the equipment used during sample processing. For cellular uptake experiments, the limit of quantitation (LOQ) for platinum was determined to be 34 ng/L and 88 ng/L for ruthenium. HeLa cells (1 x 10^6) were seeded into 75 cm^2 dishes (Thermo Scientific Nunc™), and at the exponential phase of growth, cells were treated with complex 1 or CDDP at

equimolar concentrations of 10 μM. Following 4 h and 20 h of continuous treatment, attached cells were harvested by scraping, washed by ice cold PBS and cell pellet was collected by centrifugation at 2000 rpm, 10 min. Due to the considerable detachment of treated cells (> 90%), following 20 h complex 1 incubation, detached cells were also collected for examination of Ru(II)/Pt(II) total intracellular accumulation and DNA-binding.

For verification measurements of Ru and Pt on ICP-MS were made two sets of controls (intracellular and DNA). On each pair of control, and complex Pt and Ru is spiked, respectively. As for the samples, after total mineralization and the dilution in the volumetric flask to 10 mL, the expected concentration in the solution of Pt was 0.100 mg/L, and Ru was 0.200 mg/L. Recovery rate for Pt was 101 ± 3%, and for 98 ± 4% of Ru.

2.13. Sample preparation for the measurement of DNA-binding using ICP-MS

Binding of **C1** to cellular DNA was analyzed in HeLa cells, using inductively coupled plasma mass spectrometry (ICP-MS). HeLa cells were prepared and cell pellet collected using the same procedure as described above [49, 50]. Total DNA was isolated using TRI Reagent® (Sigma Aldrich), according to the manufacturer's procedure and concentrations were determined spectrophotometrically by measuring absorbances (Eppendorf BioPhotometer 6131).

3. Results and Discussion

3.1. Synthesis and characterization of the complexes

All complexes were synthesized following the synthetic routes described in Scheme 1. The resulting complexes were found to be soluble in DMSO and DMF and to be partially soluble in methanol and acetone. All complexes were characterized by ^{1}H and ^{13}C NMR, IR, elemental analysis and mass spectrometry.

In the ^{1}H and ^{13}C NMR spectra of the complexes, all protons and carbons appear at chemical shifts expected for such types of compounds. Importantly, as determined by the integrals of the ^{1}H NMR spectra, the arene to Me_2dppz/aip ratio was found to be 1:1. This suggests a piano-stool geometry for the complexes with a coordinated chloride ligand. This

assumption is confirmed by analysis of the ESI-MS spectra, where a single peak for the products was detected corresponding to the complexes without a counterion PF_6^-.

Insert Scheme 1

3.2. Stability of the complexes in DMSO

Since all complexes were found to be well soluble in DMSO, stock solutions for IC_{50} were prepared in this solvent. In these experimental conditions, the chloride ligand of the Ru(II) arene complexes could undergo a ligand exchange with the DMSO molecule leading potentially to problems during the IC_{50} value determination [51]. For this reason, we first explored the stability of all complexes in DMSO-d6 solutions using ^{1}H NMR spectroscopy. We followed the changes in the spectra of the complexes over 48 h. The signals of the ligand did not change over time, and this for all complexes. This observation clearly indicates that the complexes are stable in DMSO.

3.3. Conductivity measurements

To further confirm that the complexes are stable over time in DMSO, conductivity measurements were carried out immediately after dissolution in DMSO and after 24 h. The conductivity values were unchanged after 24 h, and suggested existence of one cation and one anion, or 1:1 type electrolyte, by literature data [52]. Conductivity values for 1 mM solutions of complexes **1**, **2** and **3** were 40.5, 36.6 and 35.5 Ω^{-1} cm^2 mol^{-1}, respectively.

3.4. Resazurin assay

The cytotoxicity of the three new complexes **1**-**3** as well as of the free ligands was studied in three human cancer cell lines, namely human lung carcinoma (A549), human mammary gland breast adenocarcinoma (MDA-MB-231), human cervix adenocarcinoma (HeLa) and in one non-tumor human fetal lung fibroblast cell line (MRC-5). The starting ruthenium(II)-dimers and the well-known chemotherapeutic agent cisplatin were also tested as reference compounds. As shown in Table 1, all starting compounds (dimers and ligands) were found to be non-toxic in all cell lines studied in this work. Interestingly, a similar behavior was observed for complex **2**. This observation is in agreement with a previous report describing the cytotoxicity of ruthenium complexes containing different η^6-arene ligands [53]. On the contrary, complexes **1** and **3**, which contain both the *p*-cymene ligand, were found to be extremely toxic against all tested cells.

Importantly, these two complexes were found to be more cytotoxic than cisplatin. Of note, ruthenium-arene complexes with carbene ligands complexes were found to be also extremely active against cancer cells although they were not containing any intercalating ligands [54]. Nonetheless, since complex **1** was found to be the most cytotoxic complex of the series studied in this work, it was used for all following biological studies presented below. Of note, HeLa cells were chosen for all further biological studies since they showed the highest sensitivity to the action of complex **1** (IC_{50}=0.6 ± 0.5). It has to be noted that the chloride ligand in complex **1** may rapidly hydrolyse and generate an aqua complex. This mechanism is usually considered as the necessary step prior to reaction of complex with biological targets in cell [55, 56].

Insert Table 1

3.5. Cell cycle analysis

To investigate whether complex **1** interferes with cell cycle progression, flow cytometry analysis of cell cycle phase distribution was examined in HeLa cells using propidium iodide (PI) staining. The effects of complex **1** and cisplatin were analyzed at two concentrations (IC_{50} and 2 x IC_{50}) and two time points (24 h and 48 h). The results are presented in Figure 2. Following 24 h incubation, complex **1** caused changes characterized by gradual loss of cells in the G1 phase and accumulation of cells in the G2-M phase. After prolonged treatment (48 h) complex **1** caused delay in the S phase of the cell cycle, observed in a concentration dependent manner, 17.1% and 21 %, at IC_{50} and 2 x IC_{50}, respectively, compared to the control (12.9 %). Subsequently, there was accumulation of cells in the sub-G1 fraction, which increased with concentration, up to 24.5% (at 2 x IC_{50}) (Figure 2), and was higher than that caused by cisplatin (16.4%). The generation of a sub-G1 peak is considered as a hallmark of cleaved DNA in cells that underwent cell death [57, 58]. Polypyridyl aromatic derivatives and their metal complexes have been extensively described in literature as strong DNA intercalators [30, 32]. However, ruthenium complexes carrying polypyridyl-ligands may catalyze DNA cleavage by means of different mechanisms, including direct binding and conformational distortion, by topoisomerase inhibition, indirectly by reactive oxygen species (ROS) induction, or by photocleavage [59, 60, 61, 62, 63]. Increase of sub-G1 DNA-content caused by cisplatin represents apoptotic DNA fragmentation. This observation is in agreement with established literature on the mechanism of action of CDDP [64, 65, 66]. Internucleosomal-DNA fragmentation appeared in the course of

apoptotic cell death, triggered by non-reparable cisplatin-DNA adducts. The changes in the cell cycle caused by complex **1** strongly suggest that direct DNA binding of complex **1** occurred in a concentration- and time-dependent manner. These results are in agreement with previous literature reports on the ruthenium compounds carrying dipyridophenazine (dppz) derivative, which were shown to act as strong cytotoxic and DNA binding agents [67].

Insert Figure 2

3.6. Results of Annexin-FITC apoptosis assay

The potential of complex **1** or cisplatin to induce apoptosis in HeLa cells was analyzed by flow cytometry and Annexin-FITC/propidium iodide staining. The data obtained are presented in Figure 3 as a percentage of early apoptotic cells [FITC(+)PI(-)], necrotic cells [FITC(+)/PI(+)] and dead cells [FITC(-)/PI(+)]. The results show that complex **1** did not initiate phosphatidylserine externalization, which is a characteristic of apoptotic changes since (FITC+PI-) staining had a level comparable to the control at both 24 h and 48 h of drug incubation. Under the same treatment conditions, cisplatin, which was used as reference compound, caused increase of FITC(+)PI(-) staining (early apoptosis), up to 22.6% (24 h) and 10.8% (48 h). Necrotic changes, FITC(+)/PI(+), following complex **1** action were not observed and were at levels comparable to the control.

Insert Figure 3

3.7. Results of morphological analysis of cell death

Fluorescent microscopy and acridine orange/ethidium bromide (AO/EB) staining were used to analyze morphological characteristics of cell death [68]. Microphotographs of HeLa cells stained by AO/EB, following 48 h treatment with complex **1** or cisplatin, are presented in Figure 4. Non-treated cells (control cells) are dense, light green colored and elongated with spindle-shape. Only after prolonged treatment (48 h), with lower concentration (IC_{50}) of complex **1**, certain morphological changes appeared. Namely, cells started to lose their normal morphology and became rounded, reduced in size, with condensed and eccentrically located nuclei and with still intact cell membrane, since cells incorporated only AO (green fluorescence). At a higher concentration of complex **1** ($2 \times IC_{50}$), the number of cells was markedly reduced compared to

the control as many of them detached. Among the cells attached, we observed some with necrotic morphology (i.e. cells were orange-colored due to disrupted cell membrane). Switch from apoptosis to cell death morphologies with necrotic features was previously described in literature [68, 69, 70] as onset of necrotic cell changes may result from a variety of stimuli, including inactivation of certain enzymes, cell energy deprivation (ATP decrease), or ligand binding to specific plasma membrane receptors. Additional studies will however be necessary to precisely address the mechanism of cytotoxic action of complex **1**.

Insert Figure 4

3.8. ICP-MS measurement of intracellular accumulation

One of the major goals in the development of novel metal-based anticancer drug candidates is to obtain an efficient uptake of the metal into tumor cells, thereby increasing therapeutic efficacy and decreasing toxicity for healthy tissue. In order to assess how efficiently complex **1** was taken up by HeLa cells, we used inductively coupled plasma mass spectrometry (ICP-MS) [71]. Importantly, we compared this uptake with cisplatin (CDDP). Figure 5 summarizes the intracellular content (ng metal/10^6 cells) following 4 h or 20 h treatment, with equimolar concentrations, 10 μM, of complex **1** and CDDP. Cell viability and number were determined by tripan blue assay. Measurements, following 20 h of complex **1** action, were performed in the adherent cells (5.6%) and cells detached from surface, which represented more than 90 % of the assayed sample. At the same treatment conditions, cisplatin did not cause cell detachment in a significantly higher level compared to the control. It should be noted that changes in HeLa cells viability, that occurred 20 h after administration of complex **1** (10 μM), were characterized by significant cell detachment, which is also characteristics of cells dying by apoptosis [72, 73]. Moreover, as already described in literature [74, 32] biological action of ruthenium (II) complexes carrying large and rigid aromatic ligands such as dipyridophenazine (dppz), may involve interactions with cell membranes, with consequent modification of cell membrane function and cell adhesion properties. Thus, in order to obtain complete data of distribution of ruthenium complex **1** in HeLa cells, we considered that both adherent viable cells, TP(-), and detached cells, TP(+), should be analyzed by ICP-MS. As can be seen Figure 5, the total ruthenium accumulation increased in a time- and concentration-dependent manner.

Importantly in the context of anticancer drug research, complex **1** accumulated in cells more efficiently than cisplatin. Uptake of complex **1** (ng Ru/10^6 cells) following short-term treatment (4 h), 110.5 ± 0.8, was approximately 17-fold higher than cisplatin uptake (6.5 ± 0.1 ng Pt/10^6 cells). After 20 h incubation, the accumulation rate of complex **1** (ng Ru/10^6 cells), in detached cells, 175.6 ± 0.8, exceeded the one of cisplatin (8 ± 0.1 ng Pt/10^6 cells) by approximately 20-fold. However, complex **1** concentration in the adherent cells, 85.4 ± 1.1 ng Ru/10^6 cells, seemed to decrease over time. This observation could be explained if cell division took place, in this small percentage (5.6%) of treated cells, even though they were under strong cytotoxic stress.

All in all, these results clearly indicate an enhanced pattern of cellular uptake in HeLa cells of complex **1** compared to cisplatin. The lipophilic characteristics of aromatic ligands such as dipyridophenazine (dppz) certainly facilitate influx of the ruthenium(II) complex through cell membrane by passive diffusion [75]. However, as reported previously [76], this increase in lipophilicity may contribute to adverse biological effects such as toxicity or reduced selectivity toward cancer cells. The present study confirms that the coordination of the biologically inactive dipyridophenazine derivative (Me_2dppz) to a Ru(II)-*p*-cymene unit results in a complex with an enhanced cellular uptake and cytotoxicity compared to cisplatin.

Insert Figure 5

3.9. ICP-MS measurement of DNA binding

It is well-documented that the Pt(II) drugs have a mode of cytotoxic action related to DNA binding [64]. Ruthenium complexes might interact with DNA directly [77, 78], or may damage DNA indirectly, through induction of mitochondrial-apoptotic cell death or oxidative stress [79, 80]. In order to assess the ability of complex **1** to bind to DNA in HeLa cells, the amount of ruthenium bound to DNA was determined by ICP-MS following 4 h and 20 h treatment. Following prolonged action of complex **1** (20 h), measurements were performed in cells attached and cells detached, as described above. For this purpose, cells were collected immediately after treatment, and nuclear DNA was isolated and quantified. Stock solutions of DNA gave a ratio of UV absorbance A260/A280 in the range of 2.05-2.08. The results of this ICP-MS study (Figure 5) show that complex **1** binds to cellular DNA more efficiently than CDDP. The level of complex **1** binding to DNA observed after 4 h incubation, 96.4 ± 4.2 (pg

Ru/ug DNA), was much higher than DNA-platination, 16.7 ± 0.1 (pg Pt/ug DNA). With time extension, cisplatin DNA-binding increased slower than complex **1** DNA-binding. Indeed, after 20 h of incubation, the ruthenium DNA-content (pg Ru/ug DNA) measured in both cells fractions: 358.3 ± 4.6 (attached); 407.3 ± 7.7 (detached), exceeded that of cisplatin 38.4 ± 0.5 by approximately 10-fold. We may suggest that lipophilic character of complex **1** facilitates transport through the cell membrane. Once inside the cell, complex **1** enters the nucleus efficiently and reacts with nuclear DNA. ICP-MS measurement showed that ruthenium-DNA binding was comparably high in both adherent cells (TP-), and detached cells (TP+). Further study would be necessary to precisely determine if complex **1**, particularly at the high concentrations (10 μM), may also stay attached to the cell membrane and interfere to cell adhesion.

All in all, these ICP-MS results on DNA binding are in agreement with the intracellular accumulation study and the cytotoxicity data. Complex **1** enters cell faster and targets nuclear DNA more efficiently than cisplatin. This observation could be explained by controlled ligand dissociation kinetics. According to Sadler and Dyson [7, 81, 82], complexes of the type $[Ru(\eta^6\text{-}p\text{-cymene})(L)Cl]^+$ are activated to the cationic species $[Ru(\eta^6\text{-}p\text{-cymene})(L)H_2O]^{2+}$, via substitution of the chloride ligand with water. $[Ru(\eta^6\text{-}p\text{-cymene})(L)]^{2+}$ can then bind to DNA and other nucleophilic targets in the cell. In addition, we suggest that the hydrophobic/stacking interaction of the planar aromatic Me_2dppz moiety with nucleobases in DNA-helix, and the hydrophobic interaction provided by the *p*-cymene ligand, may synergistically contribute to the enhanced DNA binding affinity of the Ru(II)-arene complex cation $[Ru(\eta^6\text{-p-cymene})(L)Cl]^{2+}$ compared to cisplatin [64, 81].

4. Conclusion

In the present study, half-sandwich Ru(II)-arene complexes of the type $[(\eta^6\text{-}p\text{-cymene})Ru(Me_2dppz)Cl]PF_6$ (**1**), $[(\eta^6\text{-benzene})Ru(Me_2dppz)Cl]PF_6$ (**2**) and $[(\eta^6\text{-}p\text{-cymene})Ru(aip)Cl]PF_6$ (**3**), have been synthesized and characterized in-depth using different analytical methods. Cytotoxic activity studies on three human tumor cell lines, and one non-tumor *in vitro* cell model (MRC-5) revealed that the complexes carrying *p*-cymene as an arene, namely **1** and **3**, had a significantly higher cytotoxic activity than cisplatin, particularly in cervical (HeLa) and breast (MDA-MB-231) cancer cells. On the contrary, the corresponding

ligands did not have any cytotoxic effects (IC_{50} > 100 μM). Biological studies to unveil the mechanism of action of complex **1** revealed that this compound acts as strong a cytotoxic agent due to an efficient cellular accumulation and its ability to reach and bind nuclear DNA with a much higher affinity than cisplatin. Indeed, ICP-MS measurements showed that the cellular uptake and nuclear DNA binding of complex **1** after 4 h incubation were roughly 17- and 6- fold, respectively, higher than those of cisplatin. FACS analysis additionally indicated the ability of complex **1** to obstruct cell cycle progression in a concentration- and time-dependent manner, causing arrest in the G2-M and S phases, followed by the generation of considerable Sub-G1 DNA content (up to 24.5 % at 2 x IC_{50}, 48 h), as a hallmark of fragmented DNA. ICP-MS experiments also revealed that facile transport of the complex cation across the cell membrane, may be accounted to the hydrophobicity of both *p*-cymene and the planar aromatic Me_2dppz ligand, which, synergistically, may contribute to the DNA binding of complex **1**. For metal complexes carrying polypyridyl ligand such as dppz (complex **1**) in the present study, a DNA-based cytotoxicity may be anticipated [30, 83]. Organic agents that strongly bind DNA due to intercalation are extremely successful anticancer agents. Currently, there are several drugs (i.e Daunorubicin [84, 85, 86], Doxorubicin [21, 87, 88, 89] and Amsacrine [90, 91, 92, 93]), which are approved by the FDA for the treatment of human cancers, although with a limited range of effectiveness. In a similar line of thoughts, half-sandwich Ru(II) complexes with benzene or *p*-cymene as the arene ligand and *N*-methylhomopiperazine or *N*-methylhomopiperazine as the anthracenyl moiety were found to have an enhanced intercalation and cytotoxicity properties if the intercalative ligand possess an extended aromaticity [94]. Enhanced DNA binding of the Ru(II) compounds of the type $[Ru(\eta^6\text{-}p\text{-cymene})(L)Cl]^{2+}$ where L is a DNA intercalating ligand such as dipyridophenazine derivative (Me_2dppz), may help the development of a new family of specific DNA-targeting agents. However, as shown in this study, this strong DNA targeting can go on the expense of cancer cell selectivity. Further structure-activity study in our laboratories will be directed toward obtaining complexes with a higher selectivity.

Acknowledgments

This work was supported by the Swiss National Science Foundation Foundation (SNSF Professorships PP00P2_133568 and PP00P2_157545 to G.G.), the University of Zurich (G.G), the Stiftung für Wissenschaftliche Forschung of the University of Zurich (G.G.), the UBS

Promedica Stiftung (G.G), the Novartis Jubilee Foundation (G.G.), the COST Action CM1105 (S.N., G.G. and S.G.S.), the Swiss Government Excellence Scholarship for Postdoctoral Researcher (R.L.) and by the Ministry of Education, Science and Technological Development of the Republic of Serbia, grant numbers 172035 and III 41026 (S.N. and S.G.S.; N.G., S.A. and S. R.). We thank Biljana Dojčinović for ICP-MS measurements and Dr. Riccardo Rubbiani for helpful discussions.

References

[1] F. Muggia, Gynecol. Oncol. 112 (2009) 275-281.

[2] L. Kelland, Nat. Rev. Cancer 7 (2007) 573-584.

[3] C. G. Hartinger, N. Metzler-Nolte, P. J. Dyson, Organometallics 31 (2012) 5677-5685.

[4] G. Gasser, N. Metzler-Nolte, Curr. Opin. Chem. Biol. 16 (2012) 84-91.

[5] M. A. Jakupec, M. Galanski, V. B. Arion, C. G. Hartinger, B. K. Keppler, Dalton Trans. (2008) 183-194.

[6] G. Gasser, I. Ott, N. Metzler-Nolte, J. Med. Chem. 54 (2011) 3-25.

[7] A. A. Nazarov, C. G. Hartinger, P. J. Dyson, J. Organomet. Chem. 751 (2014) 251-260.

[8] S. M. Meier, M. Novak, W. Kandioller, M. A. Jakupec, V. B. Arion, N. Metzler-Nolte, B. K. Keppler, C. G. Hartinger, Chem. Eur. J. 19 (2013) 9297-9307.

[9] A. Bergamo, C. Gaiddon, J.H. Schellens, J.H. Beijnen, G. Sava, J. Inorg. Biochem. 106 (2012) 90-99.

[10] P. Heffeter, K. Bock, B. Atil, M. A. R. Hoda, W. Korner, C. Bartel, U. Jungwirth, B. K. Keppler, M. Micksche, W. Berger, G. Koellensperger, J. Biol. Inorg. Chem. 15 (2010) 737-748.

[11] M. Groessl, O. Zava, P. J. Dyson, Metallomics 3 (2011) 591-599.

[12] R. Trondl, P. Heffeter, C.R. Kowol, M.A. Jakupec, W. Bergerbd, B.K. Keppler, Chem. Sci. 5 (2014) 2925-2932.

[13] C. G. Hartinger, M. A. Jakupec, S. Zorbas-Seifried, M. Groessl, A. Egger, W. Berger, H. Zorbas, P. J. Dyson, B. K. Keppler, Chem. Biodivers. 5 (2008) 2140-2155.

[14] C. G. Hartinger, S. Zorbas-Seifried, M. A. Jakupec, B. Kynast, H. Zorbas, B. K. Keppler, J. Inorg. Chem. 100 (2006) 891-904.

[15] T. Gianferrara, I. Bratsos, E. Alessio, Dalton Trans. (2009) 7588-7598.

[16] A.Weiss, R. H. Berndsen, M. Dubois, C. Muller, R. Schibli, A. W. Griffioen, P. J. Dyson, P. Nowak-Sliwinska, Chem. Sci. 5 (2014) 4742-4748.

[17] Z. Adhireksan1, G. E. Davey1, P. Campomanes, M. Groess, C. M. Clavel, H. Yu, A. A. Nazarov, C. H. F. Yeo, W. H. Ang, P. Dröge, U. Rothlisberger, P. J. Dyson, C. A. Davey, Nat. Commun. 5 (2014) 4462/1-4462/13.

[18] C. Mari, V. Pierroz, S. Ferrari, G. Gasser, Chem. Sci. 6 (2015) 2660-2686.

[19] H.-K. Liu, P. J. Sadler, Acc. Chem. Res. 44 (2011) 349-359.

[20] W. M. Motswainyana, P. A. Ajibade, Adv. Chem. 2015 (2015) ID 859730.

[21] G. Lenglet, M.-H. D.-Cordonnier, J. Nucleic Acids 2010 (2010) ID 290935.

[22] H. Chen, J. A. Parkinson, S. Parsons, R. A. Coxall, R. O. Gould, P. J. Sadler, J. Am. Chem. Soc. 124 (2002) 3064- 3082.

[23] M. Castellano-Castillo, H. Kostrhunova, V. Marini, J. Kasparkova, P. J. Sadler, J.-M. Malinge, V. Brabec, J. Biol. Inorg. Chem. 13 (2008) 993-999.

[24] H.-K. Liu, J. A. Parkinson, J. Bella, F. Wang, P. J. Sadler, Chem. Sci. 1 (2010) 258-270.

[25] A. M. Pizarro, Peter J. Sadler, Biochimie. 91 (2009) 1198–1211.

[26] H. Chen, J. A. Parkinson, O. Nováková, J. Bella, F. Wang, A. Dawson, R. Gould, S. Parsons, V. Brabec, P. J. Sadler, Proc. Nat. Acad. Sci. 100 (2003) 14623-14628.

[27] M. M.-Alonso, N. Busto, F. A. Jalón, B. R. Manzano, J. M. Leal, A. M. Rodríguez, B. García, G. Espino, Inorg. Chem. 53. (2014) 11274-11288.

[28] S.T. Mutter, J. A. Platts, J. Phys. Chem. A 115 (2011) 11293-11302.

[29] F. Caruso, E. Monti, J. Matthews, M. Rossi, M. B. Gariboldi, C. Pettinari, R. Pettinari, F. Marchetti, Inorg. Chem. 53 (2014) 3668-3677.

[30] S. Schäfer, I. Ott, R. Gust, W. S. Sheldrick, Eur. J. Inorg. Chem. 19 (2007) 3034-3046.

[31] A. Frodl, D. Herebian, W. S. Sheldrick, J. Chem. Soc., Dalton Trans. (2002) 3664-3673.

[32] U. Schatzschneider, J. Niesel, I. Ott, R. Gust, H. Alborzinia, S. Wölfl, ChemMedChem 3 (2008) 1104-1109.

[33] Q. Wu, C.Fan, T. Chen, C. Liu , W. Mei, S. Chen, B. Wang, Y. Chen, W. Zheng, Eur. J. Med. Chem. 63 (2013) 57-63.

[34] C. Fan, Q. Wu, T. Chen, Y. Zhang, W. Zheng, Qi Wang, Wenjie Mei, Med. Chem. Commun. 5 (2014) 597–602.

[35] Q. Zhou, W. Lei, Y. Chen, C. Li, Y. Hou, B. Zhang, X. Wang, Chem. Eur. J. 18 (2012) 8617 – 8621.

[36] J. Valladolid, C. Hortigüela, N. Busto, G. Espino, A. M. Rodríguez, J. M. Leal, F. A. Jalón, B. R. Manzano, A. Carbayo, B. García, Dalton. Trans. 43 (2014) 2629-2645.

[37] Z. J. Li, Y. Hou, D.-A. Qin, Z.-M. Jin, M. L. Hu, PLoS One 10 (2015) e0120211.

[38] X. Duan, D. Liu, C. Chan, W. Lin, Small 11 (2015) 3962-3972.

[39] R. D. Gillard, R. E. E. Hill, R. Maskill, J. Chem. Soc. A (1970) 1447-1451.

[40] C. M. Dupureur, J. K. Barton, Inorg. Chem. 36 (1997) 33-43.

[41] J. E. Dickeson, L. A. Summers, Aust. J. Chem. 23 (1970) 1023-1027.

[42] P. Nagababu, M. Shilpa, B. Mustafa, P. Ramjee, S. Satyanarayana, in Inorganic Reaction Mechanisms, ed. I. Ivanovic-Burmazovic, De Gruyter 6 (2008) 301-311.

[43] S. B. Jensen, S. J. Rodger, M. D. Spicer, J. Organomet. Chem. 556 (1998) 151-158.

[44] W. Strober, Trypan Blue Exclusion Test of Cell Viability, Current Protocols in Immunology, Appendix 3, page B.1 (1987).

[45] M. G. Ormerod, Analysis of DNA-general methods, in: M.G. Ormerod (Ed.), Flow Cytometry, a Practical Approach, Oxford University Press, New York (1994) 119-125.

[46] M. van Engeland, L. J. W. Nieland, F. C. S. Ramaekers, B. Schutte, C. P. M. Reutelingsperger, Cytometry 31 (1998) 1-9.

[47] K. Liu, P. C. Liu, R. Liu, X. Wu, Med Sci. Monit. Basic Res. 21 (2015) 15-20.

[48] H. Gehrke, J. Pelka, Hartinger, C. G. Blank, H. Bleimund, F. Schneider, R. Gerthsen, D. Bräse, S. Crone, M. Türk, D. Marko, Arch. Toxicol. 85 (2011) 799-812.

[49] S. A. Miller, D. D. Dykes, H. F. Polesky, Nucleic. Acids. Res. 16 (1988) 1215.

[50] E. Malisić, R. Janković, Jakovljević, K. Arch. Gynecol. Obstet. 286 (2012) 723-728.

[51] M. Patra, T. Joshi, V. Pierroz, K. Ingram, M. Kaiser, S. Ferrari, B. Spingler, J. Keiser, G. Gasser, Chem. Eur. J. 19 (2013) 14768-14772.

[52] W. J. Geary, Coord. Chem. Rev. 7 (1971) 81-122.

[53] Y. K. Yan, M. Melchart, A. Habtemariam, P. J. Sadler, Chem. Comm. (2005) 4764-4776.

[54] F. Hackenberg, H. Müller-Bunz, R. Smith, W. Streciwilk, X. Zhu, M. Tacke Organometallics 32 (2013) 5551-5560.

[55] E. Sija, C. G. Hartinger, B. K. Keppler, T. Kiss, E. A. Enyedy, Polyhedron 67 (2014) 51-58.

[56] C. Scolaro, C. G. Hartinger, C. S. Allardyce, B. K. Keppler, P. J. Dyson, J. Inorg. Biochem. 102 (2008) 1743-1748.

[57] X. Huang, H. D. Halicka, F.Traganos, T.Tanaka, A. Kurose, Z. Darzynkiewicz, Cell Proliferat. 38 (2005) 223-243.

[58] E. H. Vock, W. K. Lutz, P. Hormes, H. D. Hoffmann, S. Vamvakasa, Mutat. Res. 413 (1998) 83-94.

[59] N. J. Wheate, C. R. Brodie, J. G. Collins, S. Kemp, J. R. Aldrich-Wright, Mini Rev. Med. Chem. 7 (2007) 627-648.

[60] B. R. Williams, S. R. Dalton, M. Skiba, S. E. Kim, A. Shatz, P. J. Carroll, S. J. Burgmayer, Inorg. Chem. 51 (2012) 12669-12681.

[61] M. H. Lim, H. Song, E. D. Olmon, E. E. Dervan, J. K. Barton, Inorg. Chem. 48 (2009) 5392-5397.

[62] Y. J. Liu, C. H. Zeng, Z. H. Liang, J. H. Yao, H. L. Huang, Z. Z. Li, F. H. Wu, Eur. J. Med. Chem. 45 (2010) 3087-3095.

[63] B. M. Blunden, M. H. J. Stenzel, J. Chem. Technol. Biotechnol. 90 (2014) 1177-1195.

[64] D. Wang, S. J. Lippard, Nat. Rev. Drug. Discov. 4 (2005) 307-320.

[65] R. C. Todd, S. J. Lippard, Metallomics 1 (2009) 280-291.

[66] S. Manić, L. Gatti, N. Carenini, G. Fumagalli, F. Zunino, P. Perego, Curr. Cancer Drug Targets, 3 (2003) 21-29.

[67] V. Pierroz, T. Joshi, A. Leonidova, C. Mari, J. Schur, I. Ott, L. Spiccia, S. Ferrari, G. Gasser, J. Am. Chem. Soc. 134 (2012) 20376-20387.

[68] A. Savić, L. Filipović, S. Aranđelović, B. Dojčinović, S. Radulović, T.J. Sabo, S. Grgurić-Šipka, Eur. J. Med. Chem. 82 (2014) 372-384.

[69] L. Gallussi, G. Kroemer, Cell 135 (2008) 1161-1163.

[70] S. M. Sancho-Martínez, F. J. Piedrafita, J. B. Cannata-Andía, J. M. López-Novoa, F. J. López-Hernández, Toxicol. Sci. 122 (2011) 73-85.

[71] I. Ott, C. Biot., C. G. Hartinger; *AAS, XRF and MS Methods in Chemical Biology of Metal Complexes*, *Vol.* (Ed. G. Gasser), Wiley-VCH Verlag GmbH & Co. KGaA (2014) 63-97.

[72] G. Kroemer, L. Galluzzi, P. Vandenabeele, J. Abrams, E.S. Alnemri, E.H. Baehrecke, M.V. Blagosklonny, W.S. El-Deiry, P. Golstein, D.R. Green, M. Hengartner, R.A. Knight, S. Kumar, S.A. Lipton, W. Malorni, G. Nun˜ez, M.E. Peter, J. Tschopp, J. Yuan, M. Piacentini, B. Zhivotovsky, G. Melino, Cell Death Differ. 16 (2009) 3-11.

[73] J. Grossmann, K. Walther, M. Artinger, S. Kiessling, J. Schölmerich, Cell Growth Differ. 12 (2001) 147–155.

[74] T. Gianferrara, I. Bratsos, E. Alessio, Dalton Trans. (2009) 7588-7598.

[75] C. A. Puckett, J. K. Barton, Biochem. 47 (2008) 11711-11716.

[76] H. Huang, P. Zhang, B. Yu, Y. Chen, J. Wang, L. Ji, H. Chao, J. Med. Chem. 57 (2014) 8971-8983.

[77] O. Novakova, J. Kasparkova, V. Bursova, C. Hofr, M. Vojtiskova, H. Chen, P. J. Sadler, V. Brabec. Chem. Biol. 12 (2005) 121-129.

[78] V. Brabec, O. Nováková, Drug. Resist. Update 9 (2006) 111-122.

[79] C. Qian, J. Q. Wang, C. L. Song, L. L. Wang, L. N. Ji, H. Chao, Metallomics 5 (2013) 844-854.

[80] V. Vidimar, X. Meng, M. Klajner, C. Licona, L. Fetzer, S. Harlepp, P. Hebraud, M. Sidhoum, C. Sirlin, J. P. Loeffler, G. Mellitzer, G. Sava, M. Pfeffer, C. Gaiddon, Biochem. Pharmacol. 84 (2012) 1428-1436.

[81] T. Bugarčić, A. Habtemariam, R. J. Deeth, F. P. A. Fabbiani, S. Parsons, P. J. Sadler, Inorg. Chem. 48 (2009) 9444–9453.

[82] S. Betanzos-Lara, A. Habtemariam, G.J. Clarkson, P.J. Sadler, Eur. J. Inorg. Chem. 21 (2011) 3257-3264.

[83] A. Frodl, D. Herebian, W. S. Sheldrick, J. Chem. Soc. Dalton Trans. (2002) 3664-3673.

[84] K. Klein, G. L. Kaspers, Oncol. Hemat. Rev. (US) 9 (2013) 142-148.

[85] B. Löwenberg, G. J. Ossenkoppele, W. van Putten, H. C. Schouten, C. Graux, A. Ferrant, P. Sonneveld, J. Maertens, M. Jongen-Lavrencic, M. von Lilienfeld-Toal, B. J. Biemond, E. Vellenga, M. van Marwijk Kooy, L. F. Verdonck, J. Beck, H. Döhner, A. Gratwohl, T. Pabst, G. Verhoef, N. Engl. J. Med. 361 (2009) 1235-1248.

[86] G. Aubel-Sadron, D. Londos-Gagliardi, Biochemie. 66 (1984) 333-352.

[87] H. G. Keizer, H. M. Pinedo, G. J. Schuurhuis, H. Joenje, Pharmacol. Therapeut. 47 (1990) 219-231.

[88] Y. Octavia, C. G. Tocchetti , K. L. Gabrielson, S. Janssens, H. J. Crijns, A. L. Moens, J. Mol. Cell. Cardiol. 52 (2012) 1213-1225.

[89] C. Pisano, S. C. Cecere, M. Di Napoli, C. Cavaliere, R. Tambaro, G. Facchini, C. Scaffa, S. Losito, A. Pizzolorusso, S. Pignata, J. Drug Deliv. 2013 (2013) Article ID 898146.

[90] Z. A. Arlin, E. J. Feldman, A. Mittelman, T. Ahmed, C. Puccio, H. G. Chun, P. Cook, P. Baskind, C. Marboe, R. Mehta, Cancer 68 (1991) 1198-1200.

[91] E. Berman, J. Clin. Pharmacol. 32 (1992) 296-309.

[92] W. R. Grove, C. L. Fortner, P. H. Wiernik, Clin. Pharm. 1 (1982) 320-326.

[93] P. A. Cassileth, R. P. Gale, Leuk. Res. 10 (1986) 1257-1265.

[94] M. Ganeshpandian, R. Loganathan, E. Suresh, A. Riyasdeen, M. A. Akbarshad, M. Palaniandavar, Dalton Trans. 43 (2014) 1203-1219.

Table(s)

Table 1. IC_{50} values of complexes **1-3** and of the starting ruthenium(II) dimers and ligands as well as cisplatin against different human cell lines

Compounds	IC_{50} Values (μM)			
	A549	**MDA-MB-231**	**HeLa**	**MRC-5**
[(η^6-*p*-cymene)Ru(Me_2dppz)Cl]PF_6 (**1**)	6.9 ± 2.9	0.7 ± 0.3	0.6 ± 0.5	0.4 ± 0.1
[(η^6-benzene)Ru(Me_2dppz)Cl]PF_6 (**2**)	>100	>100	>100	>100
[(η^6-*p*-cymene)Ru(aip)Cl]PF_6 (**3**)	24.5 ± 0.1	3.7 ± 0.3	4.9 ± 0.1	3.2 ± 0.1
[(η^6-benzene)$RuCl_2$]$_2$	>100	>100	>100	>100
[(η^6-*p*-cymene)$RuCl_2$]$_2$	>100	>100	>100	>100
Me_2dppz	>100	58.8	>100	>100
aip	>100	>100	>100	>100
cisplatin	28.5 ± 5.1	27.9 ± 2.7	16.4 ± 7.1	17.0 ± 6.2

Scheme 1

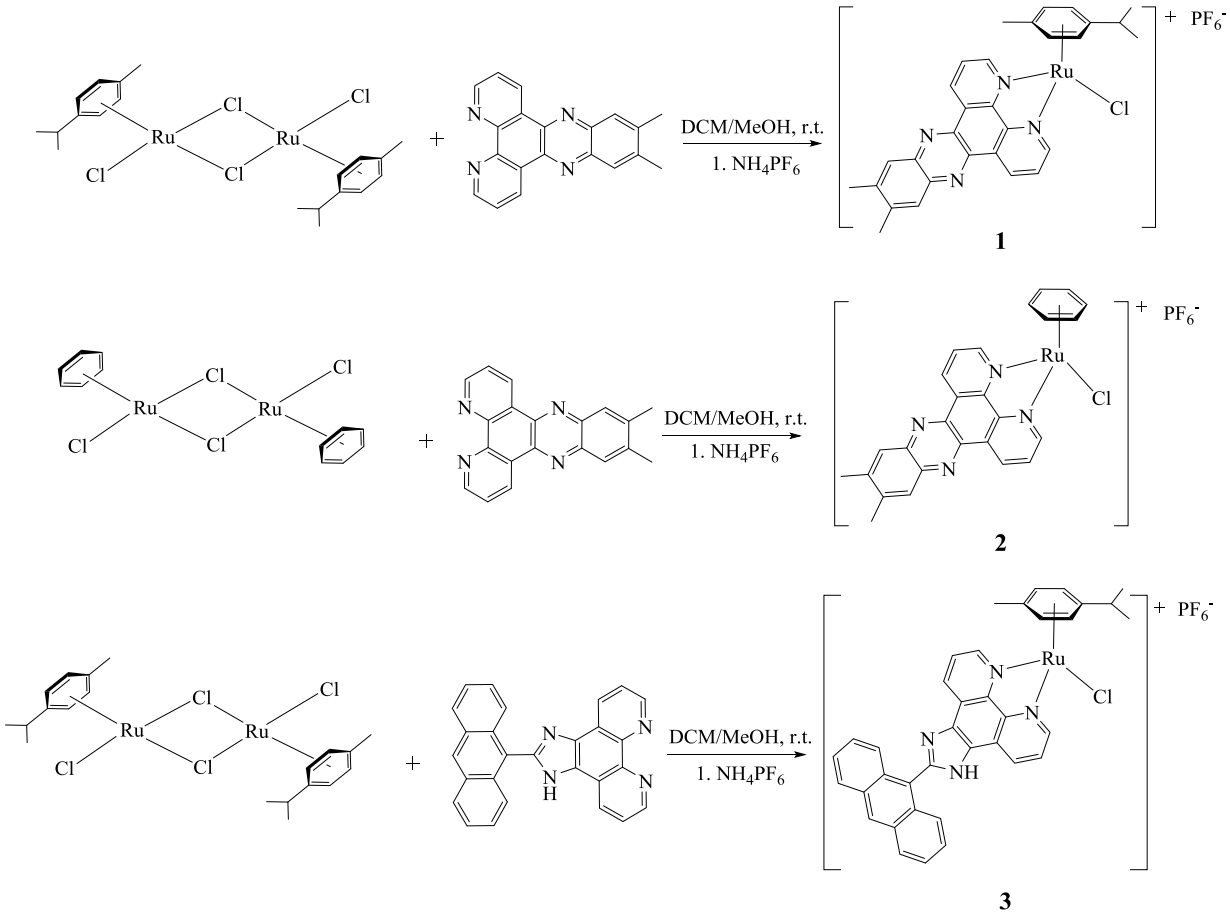

Scheme 1. Synthesis of complexes **1**- **3**.

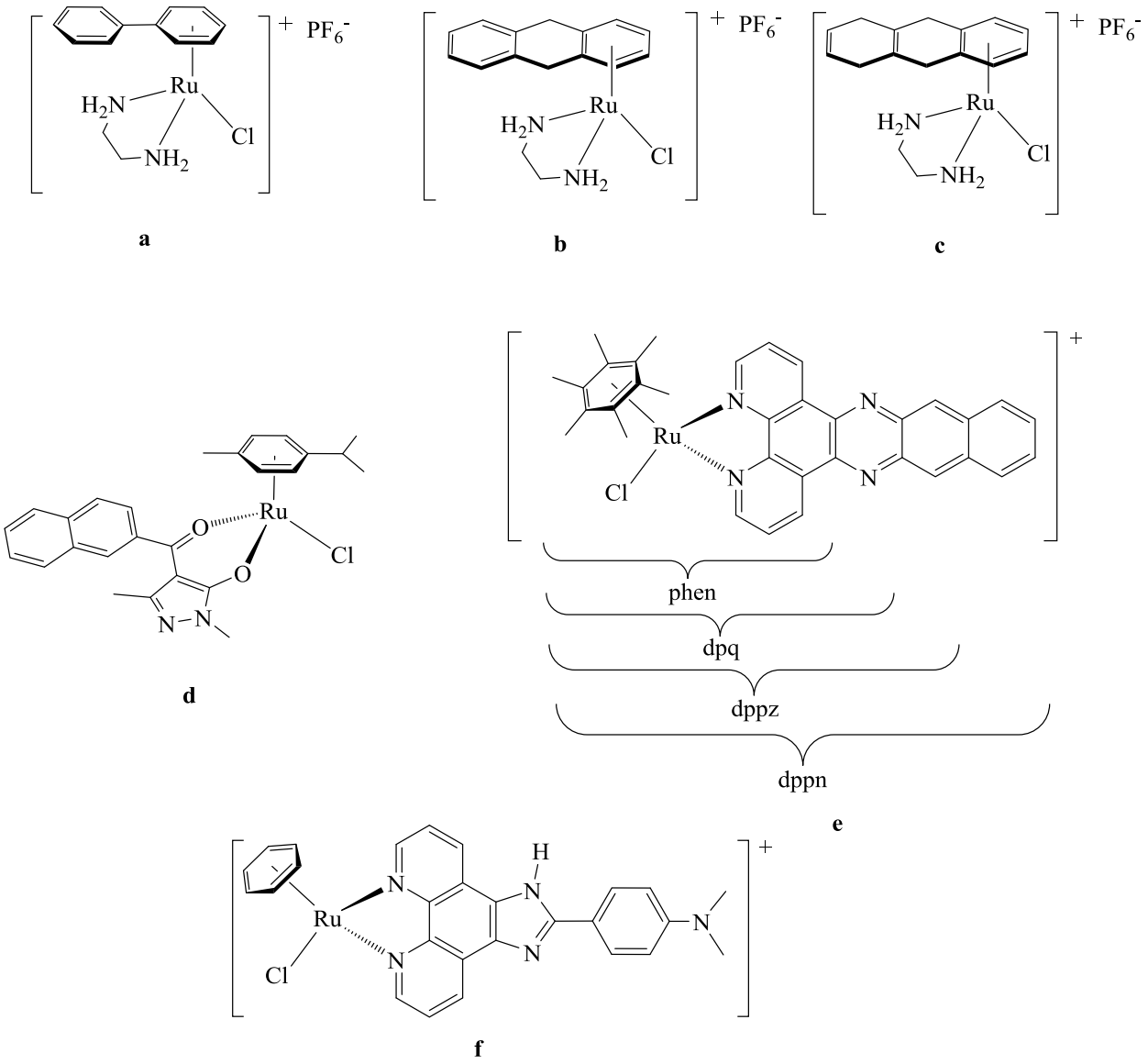

Figure 1. Examples of organometallic ruthenium complexes bearing an intercalating moiety.

Figure 2

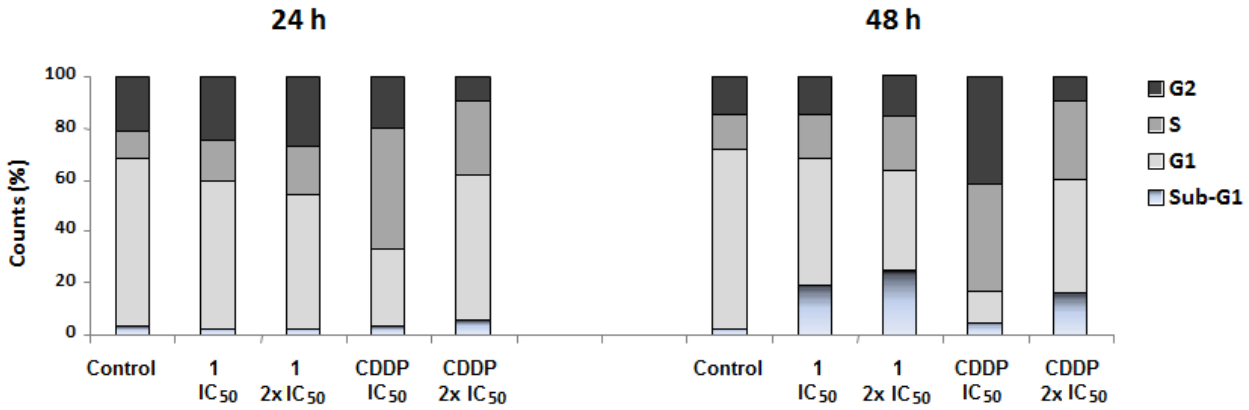

Figure 2. Diagrams presenting cell cycle phase distribution of HeLa cells, treated with complex **1** or CDDP. These results were obtained by flow-cytometric analysis of DNA content in fixed cells, after staining with PI. HeLa cells were collected following 24 or 48 h treatment, with complex **1** or CDDP, at concentrations corresponding to IC_{50} and 2 x IC_{50}. Bar graphs show representative measurements of at least three independent experiments.

Figure 3

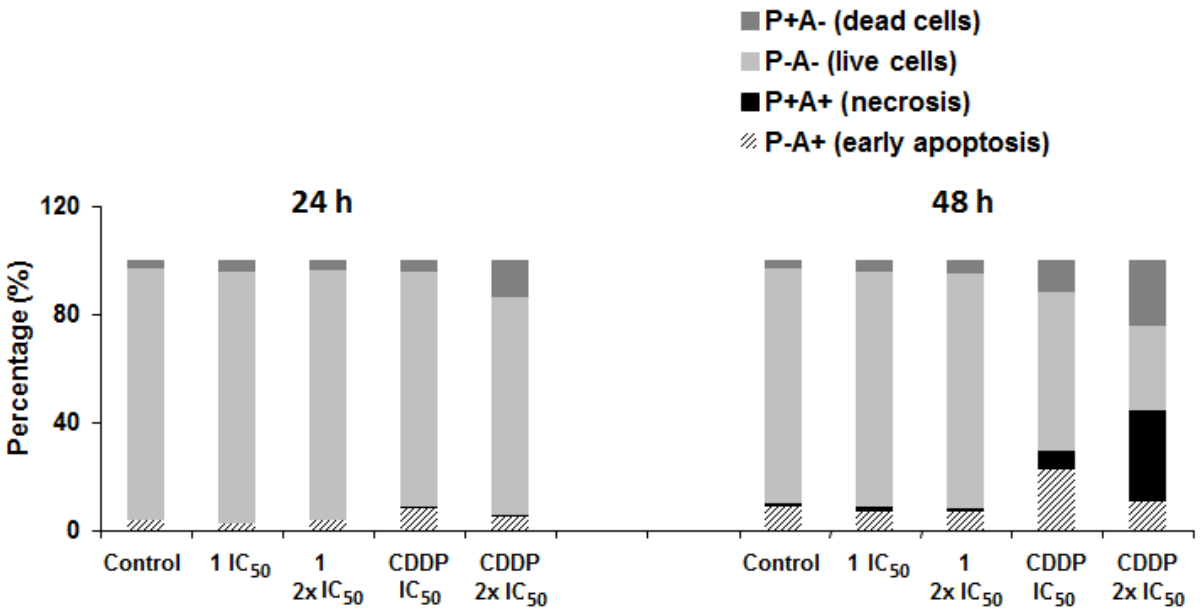

Figure 3. Diagrams show results of dual **PI/A**nnexin V-FITC staining, (abbreviated as **P/A**), monitored by FACS-flow in HeLa cells, following 24 h and 48 h treatment with complex **1** or CDDP at concentrations corresponding to IC_{50} and 2 x IC_{50}. Bar graphs present the percentage of live cells PI(-)/FITC(-); early apoptotic cells at lower-right quadrant, PI(-)/FITC(+); necrotic cells at upper-right quadrant, PI(+)/FITC(+); and dead cells at upper-left quadrant, PI(+)/FITC(-). Bar graphs represent measurements of one of at least three independent experiments.

Figure 4

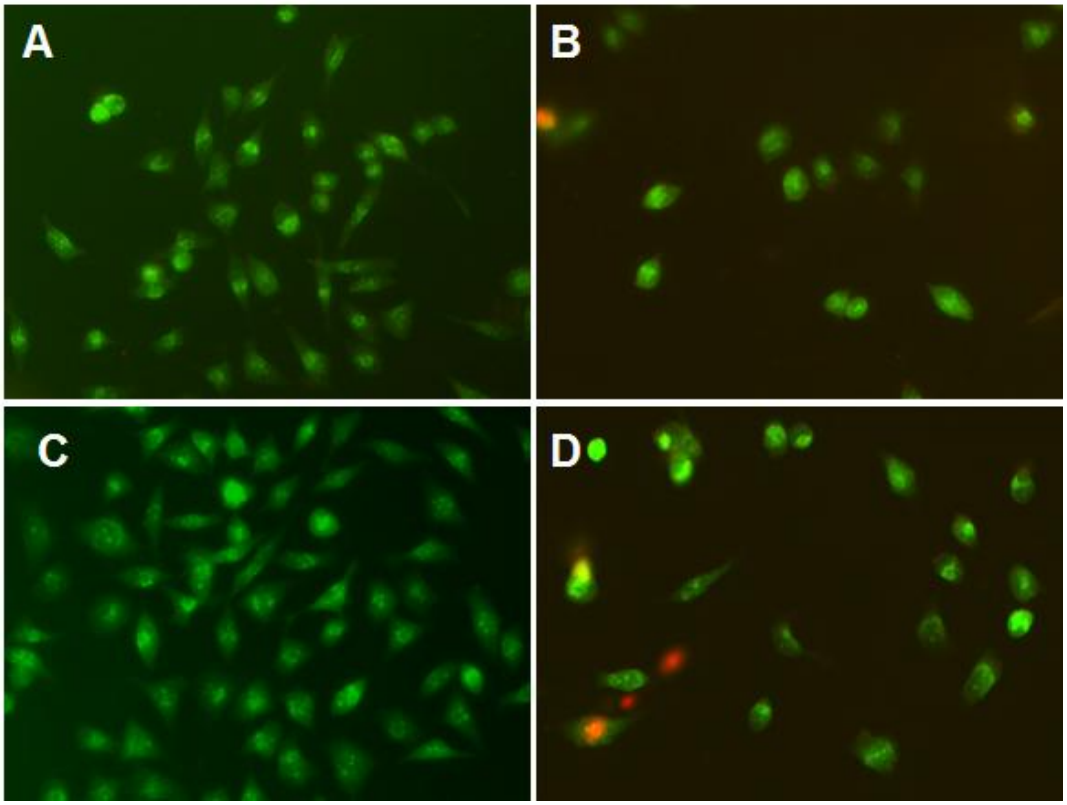

Figure 4. Fluorescent micrographs presenting HeLa cells treated with complex **1** for 48 h at concentrations corresponding to A) IC_{50} and B) 2 x IC_{50}. C) Untreated HeLa cells were used as negative control; D) HeLa cells treated with CDDP at IC_{50}, used as positive control for apoptotic morphological changes. Cell staining by Ethidium bromide (EB) and Acridine orange (AO) was analyzed using a fluorescent microscope Axio Observer Z1, using AxioVision imaging software (Carl Zeiss MicroImaging GmbH) was used. AO is a vital dye, which stains both live and dead cells. EB only stains cells that have lost membrane integrity. Untreated control cells appeared uniformly green with spindle-shape.

Figure 5

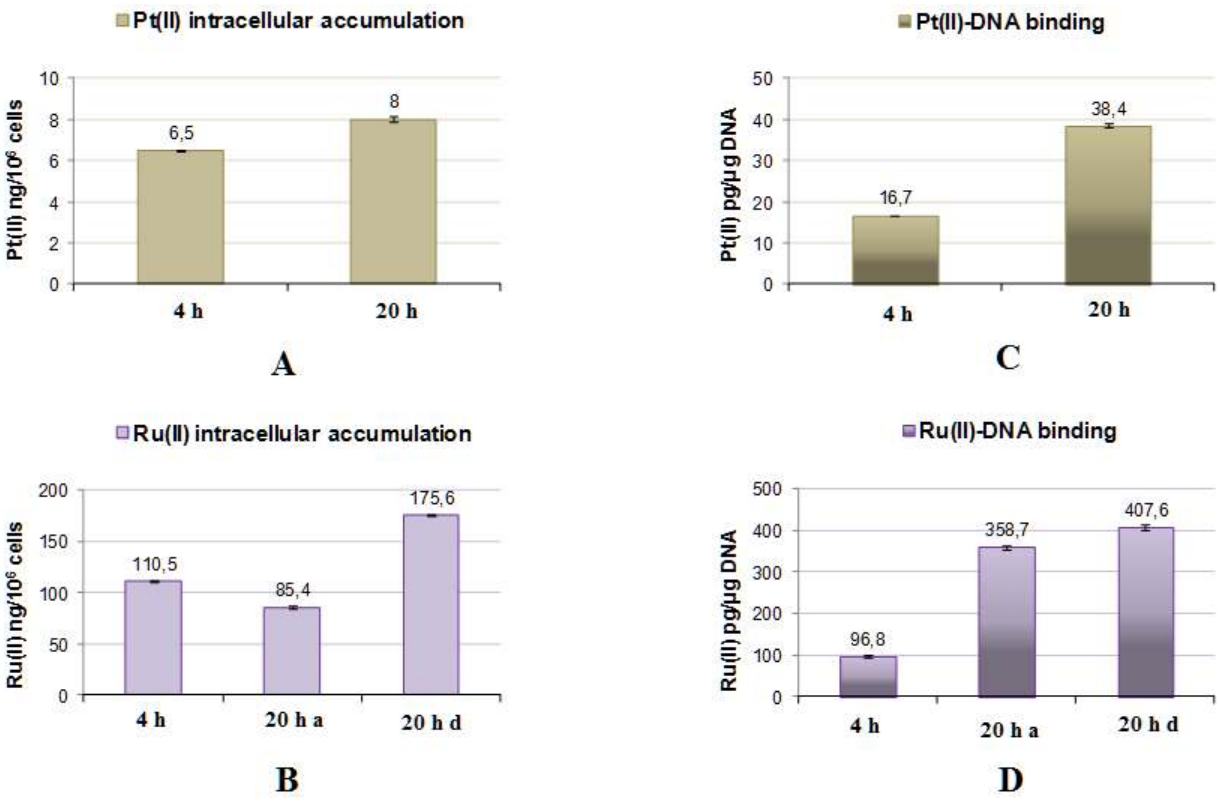

Figure 5. Results of ICP-MS analysis of complex **1**-ruthenium(II) and cisplatin-platinum(II) intracellular accumulation and DNA binding, in HeLa cells, after 4 and 20 h treatment, with 10 μM of the compounds. A) cisplatin intracellular accumulation (ng Pt(II)/10^6cells); B) complex **1** intracellular accumulation (ng Ru(II)/10^6cells); C) cisplatin-DNA binding (pg Pt(II)/μg DNA); D) complex **1**-DNA binding (pg Ru(II)/μgDNA) **a)** adherent cells, TP(-) after complex **1** action (20 h); **d)** cells detached, TP(-) after complex **1** action (20 h); Bar graphs represent mean ± SD of three independent measurements.

*Pictogram for the Graphical Abstract

Graphical Abstract